Journal of Alloys and Compounds 509 (2011) 9638–9644

Contents lists available at ScienceDirect

Journal of Alloys and Compounds

journal homepage: www.elsevier.com/locate/jallcom

Effect of Gd^{3+} doping on magnetic, electric and dielectric properties of $MgGd_xFe_{2-x}O_4$ ferrites processed by solid state reaction technique

Jagdish Chand[a,b,*], Gagan Kumar[a], Pawan Kumar[a], S.K. Sharma[c], M. Knobel[c], M. Singh[a]

[a] Department of Physics, Himachal Pradesh University, Shimla 171005, India
[b] Department of Physics, Govt. P. G. College, Solan, India
[c] Instituto de Fisica Gleb Wataghin, Universidade Estadual de Campinas (UNICAMP) Campinas 13083-859, SP, Brazil

ARTICLE INFO

Article history:
Received 3 December 2010
Received in revised form 17 July 2011
Accepted 18 July 2011
Available online 29 July 2011

PACS:
75.25.Dk
75.30.Cr
75.30.Et
75.50.Gg
75.60.−d
75.60.Ej

Keywords:
Ferrite
Saturation magnetization
Remnant magnetization
Relative loss factor
Initial permeability
Resistivity
Dielectric loss

ABSTRACT

$MgGd_xFe_{2-x}O_4$ ($x = 0.0, 0.05, 0.1$ and 0.15) ferrites, with improved dc resistivity, initial permeability, saturation magnetization, and extremely low relative loss factor, have been synthesized by solid state reaction technique. The microstructures, electric, dielectric and magnetic properties have been investigated by means of X-ray diffraction, Keithley 2611 system, impedance analyzer and VSM respectively. The addition of Gadolinium in Mg ferrite has been shown to play a crucial role in enhancing the electric, dielectric and magnetic properties. The dc resistivity is increased by two orders of magnitude as compared to Mg ferrite. Saturation magnetization has been increased by two times and remnant magnetization has been increased by more than three times due to the doping of Gd^{3+} ions in Mg ferrite. The relative loss factor was found to have very low values and is of the order of 10^{-4}–10^{-5} in the frequency range 0.1–30 MHz. The variations of electric, dielectric and magnetic properties of the samples have been studied as a function of frequency and Gd^{3+} ions concentration measured at room temperature. High resistivity and improved magnetic properties can be correlated with better compositional stoichiometry and the replacement of Fe^{3+} ions by Gd^{3+} ions. The mechanisms responsible to these results have been discussed in this paper.

1. Introduction

Ferrites have many applications in heterogeneous catalysis, magnetic materials, refractory materials, medical diagnostics, and in sensors [1]. The practical applications of ferrites are growing in leaps and bounds with the advancement in nanotechnology [2]. Spinel ferrites have been extensively investigated in recent years for their useful electrical, dielectric and magnetic properties and applications in information storage systems, magnetic bulk cores, magnetic fluids, microwave absorbers and high frequency devices [3]. The magnetic properties of the spinel ferrite depend on the distribution of cations among the two sub-lattices, tetrahedral (A) and octahedral [B] sites [4]. The excellent combination of electric, magnetic and dielectric properties of Mg ferrites can be used to fulfill the future demand for high-frequency applications [5]. The electrical and dielectric properties of Mg–Gd ferrites have showed strong dependence on structural properties. Mg–Gd ferrites have proved to be very useful in microwave applications because of their low cost, high resistivity and low eddy current loss [6]. The values of RLF in the presently studied ferrites at room temperature are of the order of 10^{-4}–10^{-5}. Low values of RLF exhibited by these ferrites suggest its utility in inductor and transformer applications [7]. The important magnetic property of ferromagnetic spinel ferrites mainly depends on the magnetic interactions between cations with magnetic moments that are situated in the tetrahedral (A) and the octahedral [B] sites [8]. In the present study, we have investigated the variation of dielectric and magnetic properties of the ferrites with frequency measured at room temperature. In addition to this, the effects of Gd^{3+} ions doping on the magnetic, dielectric and electric properties were investigated and reported in the present work.

2. Experimental details

Ferrites powder of compositions $MgGd_xFe_{2-x}O_4$ ($x = 0.0, 0.05, 0.1$ and 0.15) was prepared by solid state reaction technique. Analytical grade reagents MgO (>97%,

* Corresponding author at: Department of Physics, Himachal Pradesh University, Shimla 171005, India.
E-mail address: sonusamar8@gmail.com (J. Chand).

0925-8388/$ – see front matter © 2011 Elsevier B.V. All rights reserved.
doi:10.1016/j.jallcom.2011.07.055

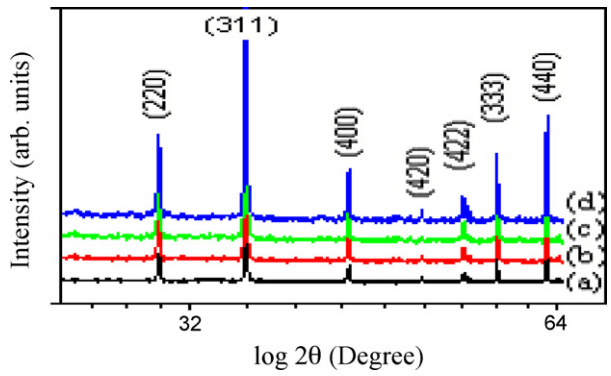

Fig. 1. XRD patterns of $MgGd_xFe_{2-x}O_4$ samples (a) x = 0.0, (b) x = 0.05, (c) x = 0.1 and (d) x = 0.15 sintered at 1273K.

Merck, India), Gd_2O_3 (>99%, Merck, Germany) and Fe_2O_3 (>98.5%, Loba chemie, India) were weighted in appropriate proportions and mixed thoroughly by wet blending with de-ionized water in an agate mortar and pestle. The powder is crushed and mixed for 5–10 h in de-ionized water to break it into small crystallites of uniform size. The mixed powders were dried and calcinated at 1073 K for 3 h to improve the homogeneity of the constituents. The rate of heating is maintained at 5.83 °C/min during samples preparation. The high rate of heating may results in production of fine grains because shrinkage occurs prior to grain growth. Initial particle size also plays an important role during sintering. The reacted material was well milled by adding a small quantity of polyvinyl alcohol as a binder, to reduce the particle size. The homogeneity of a ferrite depends on grain size, milling, calcining temperature and heating rate during sample preparation. The calcined and sintered ferrite homogeneity is correlated to the loss factor. As expected, the ferrite with the greatest homogeneity has the lowest loss factor. The loss factor decreases with an increase in Gd^{3+} ions concentration in Mg ferrite. The powders were compressed into pellets and toroids uniaxially under a pressure of 3–5 ton/in.^{2} in a stainless steel die. The powders, toroids and pellets were finally sintered at 1273 K for 3 h at a heating rate of 5.83 °C/min and slowly cool down at the rate of 1 °C/min to room temperature. The phase structure of ferrites was analyzed by XRD (Rigaku-Denki X-ray diffractometer, Japan) using Cu-K_α source. For electric and dielectric measurement both surfaces of the pellet were coated with silver paste to make electrodes. The dielectric constant, dielectric loss, initial permeability and relative loss factor were determined by Agilent Precision LCR meter (Agilent Technologies, Model HP4285A, Japan) in the frequency range 0.1–30 MHz. The dc resistivity of the sample at different temperatures was measured by using a Keithley instruments (Model 2611, USA). The magnetic hysteresis measurements have been performed using a commercial available Vibrating Sample Magnetometer (LakeShore, Model 7140, USA). For the measurements of initial permeability and relative loss factor (RLF) the toroids were wounds with 55 turns of 32 SWG (Standard Wire Gauge) enameled copper wire. The initial permeability was calculated by using the relation [9,10]

$$\mu_i = \frac{L}{L_o} \tag{1}$$

where L is the measured inductance of the sample and L_o is the inductance with air core and $L_o = 4.6N^2 d \log(OD/ID) \times 10^{-9}$ H, N being the number of turns, d is the thickness of the toroid in meter and OD and ID are the outer and inner diameters of the toroid respectively.

3. Results and discussion

3.1. Structural study

The X-ray diffraction patterns of the prepared ferrites $MgGd_xFe_{2-x}O_4$ (x = 0.00, 0.05, 0.1 and 0.15) are shown in Fig. 1. All the samples can be indexed as the single-phase cubic spinel structure. The lattice parameters of the prepared ferrites were obtained from XRD studies for various compositions of $MgGd_xFe_{2-x}O_4$ (x = 0.00, 0.05, 0.1 and 0.15) and are found to be increasing with the increasing concentration of Gd^{3+} ions. The lattice parameter a, was calculated by using the following relation

$$a = d_{h\ k\ l}(h^2 + k^2 + l^2)^{1/2}, \tag{2}$$

where the values of lattice parameter a, for each composition are calculated. The lattice parameter increases from 8.3798 Å to 8.3833 Å with an increase in Gd^{3+} ions concentration (x). Such a change in the lattice parameter is expected because Fe^{3+} ions, which are of smaller radius (0.067 nm), are being progressively replaced with Gd^{3+} ions, which are of larger size (0.0938 nm). The morphology and the size of particles of $MgGd_{0.15}Fe_{1.85}O_4$ power sintered at 1273 K were checked by SEM, shown in Fig. 2. The average particle size is about 0.1–2 μm at 1273 K. The X-ray density was calculated by using the relation

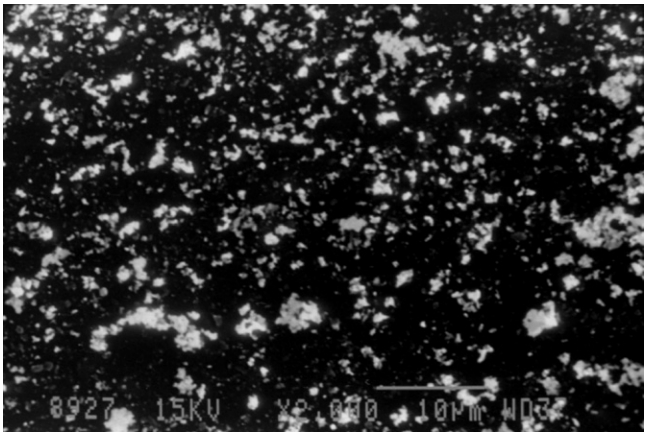

Fig. 2. SEM of $MgGd_{0.15}Fe_{1.85}O_4$ power sintered at 1273 K.

$$D_x = \frac{8M}{Na^3} \tag{3}$$

where N is the Avogadro's number, a is lattice parameter and M is the molecular weight. The values of X-ray density increases from 4.515 to 4.851 g cm^{-3} with Gd^{3+} ions concentration (x).

The real or observed density (D) of the ferrite samples is measured by using the Archimedes principle. The real density (D) is determined by using the following formula

$$D = \frac{\text{Weight of the sample in air}}{\text{Loss of weight of the sample in distilled water}} \tag{4}$$

The porosity of the samples is calculated by using the relation

$$P = \frac{1 - D}{D_x} = \frac{D_x - D}{D_x} \tag{5}$$

The variation of lattice constant, real density (D) and porosity (P) of $MgGd_xFe_{2-x}O_4$ ferrites as a function of Gd^{3+} ions concentration (x) are tabulated in Table 1. The data shows that the porosity increases with an increase in Gd^{3+} ions content. Higher porosity results in lower dielectric constants and dielectric losses [11]. The increase in porosity plays a vital role in determining the electric and dielectric properties of Gd–Mg ferrite.

3.2. Cation distribution analysis

The cation distribution in the present system is derived from site preference energies and magnetization method. According to the Neel's two sub-lattice model of ferrimagnetisms the magnetic

Table 1
Variation of lattice constant (a), real density (D) and porosity (P) of $MgGd_xFe_{2-x}O_4$ ferrite as a function of x.

Composition	Lattice constant (Å)	D (g/cm^3)	Porosity (P)
x = 0.0	8.3798	4.214	0.066
x = 0.05	8.3809	3.47	0.250
x = 0.1	8.3821	3.2928	0.3052
x = 0.15	8.3833	2.96	0.3898

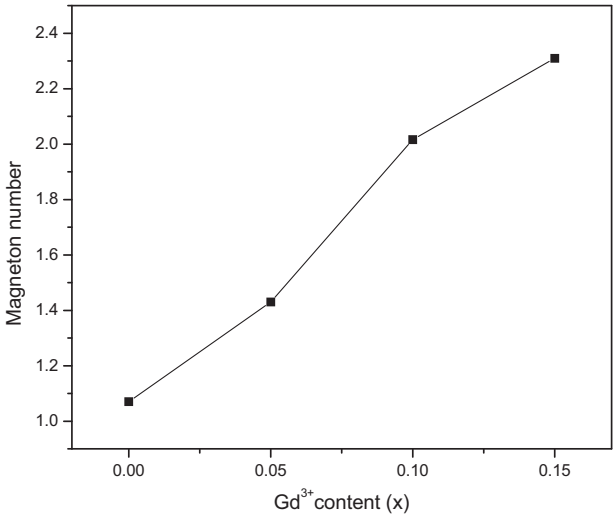

Fig. 3. Variation of magneton number (n_B^N) with Gd^{3+} ions content (x).

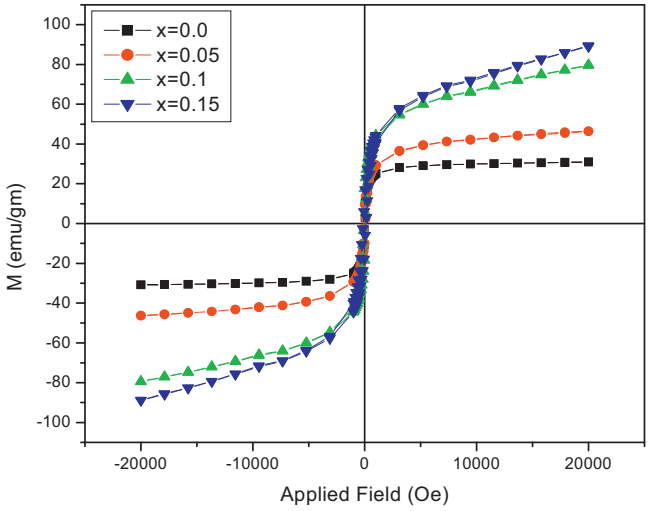

Fig. 4. Variation of magnetization of $MgGd_xFe_{2-x}O_4$ (x = 0.0, 0.05, 0.1 and 0.15) ferrites with applied field at 300 K.

moment per formula unit in Bohr magneton (μ_B); n_B^N is expressed as

$$n_B^N = M_B(x) - M_A(x), \quad (6)$$

where $M_B(x)$ and $M_A(x)$ are octahedral [B] and tetrahedral (A) sub-lattice magnetic moments in Bohr magneton. The values of magneton number n_B^N (saturation magnetization per formula unit in Bohr magneton) at room temperature were calculated, by using the relation

$$n_B^N = \frac{M_s \times M}{N n_B} \quad (7)$$

where M is the molecular weight of ferrite sample, M_s is the saturation magnetization, N is the Avogadro's number and n_B is the Bohr magneton. The n_B^N (μ_B) values were calculated by using the free ion magnetic moments of Fe^{3+}(5 μ_B), Gd^{3+}(8 μ_B) and Mg^{2+} (0 μ_B) ions. Variation of magneton number with Gd^{3+} ions content (x) is shown in Fig. 3. The ferrite in the present system is mostly inverse. The cation distribution in the present system as derived from site preference energies and magnetization method is represented as

$(Mg_{0.1}Fe_{0.893})_A[Fe_{1.107}Mg_{0.9}]_B \quad (x = 0.0)$

$(Mg_{0.127}Fe_{0.868})_A[Fe_{1.085}Gd_{0.047}Mg_{0.873}]_B \quad (x = 0.05)$

$(Mg_{0.15}Fe_{0.843})_A[Fe_{1.008}Gd_{0.149}Mg_{0.85}]_B \quad (x = 0.1)$

$(Mg_{0.19}Fe_{0.823})_A[Fe_{0.997}Gd_{0.180}Mg_{0.81}]_B \quad (x = 0.15)$

3.3. Magnetic study

Magnetic characterization of the samples was done by using vibrating sample magnetometer at room temperature with maximum applied field up to 20 kOe as shown in Fig. 4. The magnetization of Mg–Gd samples does not saturate even at the maximum field attainable (H = 20 kOe), while pure Mg ferrite sample attain saturation magnetization in the applied field. For $MgGd_xFe_{2-x}O_4$ (x = 0.0, 0.05, 0.1 and 0.15) samples the saturation magnetization, M_s is determined by extrapolating the M versus I/H curve to I/H = 0 [12]. The non-saturated magnetization suggests the existence of strong antiferromagnetic coupling between adjacent Gd^{3+}–Gd^{3+} ions mixed with ferromagnetic interactions [13–15]. The values of saturation magnetization and remnant magnetization have been increased significantly due to the doping of Gd^{3+} ions in Mg ferrite. The saturation magnetization (M_s) obtained at room temperature has been increased from 30 emu/g to 59.9 emu/g and the value of remnant magnetization (M_r) has been increased from 3.6573 emu/g to 11.674 emu/g due to the doping of Gd^{3+} ions in Mg ferrite. This increase in saturation magnetization and remnant magnetization is attributed to the magnetic interactions in ferrites. The magnetic order in the cubic ferromagnetic spinels is due to super exchange interaction mechanism occurring between the metals ions in the tetrahedral (A) and octahedral [B] sub-lattices. The A–A interactions as well as the B–B interactions exist but they are very weak. Since the A–B interactions are the strongest, it will align all the magnetic moments (spin) at the (A) site in one direction and those at [B] site in the opposite direction, thus constituting two saturated and oppositely magnetized sub-lattices at 0 K. The resultant magnetization is, therefore, the difference between the magnetization of [B] and (A) sub-lattices, the former generally having larger value. The dominant A–B interactions lead to complete or partial (non-compensated) ferrimagnetisms [16]. Thus the net saturation magnetization is given by equation:

$$M_s = M_B - M_A \quad (8)$$

The site preference of magnetic ions also depends on temperature. Some sites may particularly favor certain ions over others at high temperatures, but reverse the order of preference at low temperatures. As the samples are sintered at high temperatures, some Mg^{2+} ions goes into the tetrahedral sites leaving the remaining tetrahedral (A) sites for only part of the Fe^{3+} ions. The remainder (more than half) of the original Fe^{3+} ions goes to octahedral [B] sites. This gives rise to a magnetic moment of Mg ferrite. In case of $MgGd_xFe_{2-x}O_4$ samples the Fe^{3+} ions are replaced by the Gd^{3+} ions at the [B] site. The octahedral site preference energy is large for Gd^{3+} ($4f^7$) ions as compared to tetrahedral site preference energy. So due to the large octahedral site preference energy Gd^{3+} ions occupy [B] sites only. Since the magnetic moment of Gd^{3+} ions (8 μ_B) is more than Fe^{3+} ions (5 μ_B), a replacement of Fe^{3+} ions by Gd^{3+} ions results an increase in the magnetic moment of the magnetic ions. This results an increase in the magnetic moment at the [B] sublattice, so that the overall total magnetic moment increases. Fig. 5 shows that saturation magnetization increases with an increase in Gd^{3+} ions concentrations.

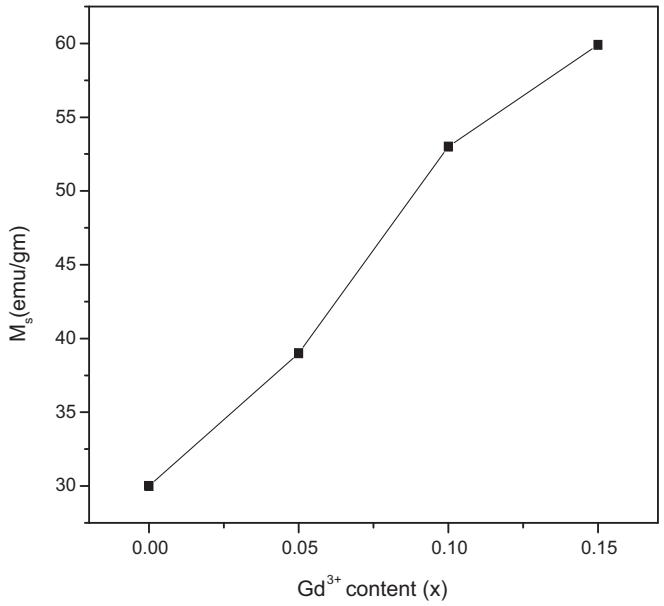

Fig. 5. Variation of saturation magnetization (M_s) with Gd^{3+} ions content (x) measured at room temperature.

3.4. Initial permeability

The variation of initial permeability (μ_i) of $MgGd_xFe_{2-x}O_4$ ferrites with frequency measured at room temperature is shown in Fig. 6. The variation of μ_i with frequency can be understood on the basis of Globus model [17,18]. According to this model, the relaxation character is,

$$(\mu_i - 1)^2 \quad f_r = \text{constant}, \tag{9}$$

where μ_i is the static initial permeability and f_r is the relaxation frequency.

It follows from the above mentioned equation that the dispersion frequency is expected to be lower for specimen of higher permeability. This is due to the fact that for materials of lower initial permeability the demagnetizing field, which appear during wall movement, results in increasing the restoring force, thereby increasing the relaxation frequency. The increase in μ_i above 15 MHz may indicate the beginning of a resonance with peaks occurring at higher frequencies. The resonance occurs due to the matching of applied field frequency with the precising frequency of magnetic spins in ferrites. This matching leads to energy transfer from the field to the ferrite system in orienting the dipoles. The result shows fairly constant values of μ_i over a wide frequency range, implying compositional stability and quality of ferrites. This is a desirable characteristic for various applications such as broadband pulse transformers and wide band read-write heads for video recording. Fig. 6 shows that the values of initial permeability increases with an increase in Gd^{3+} ions concentration. These variations can be explained from the following dependence of μ_i [19]

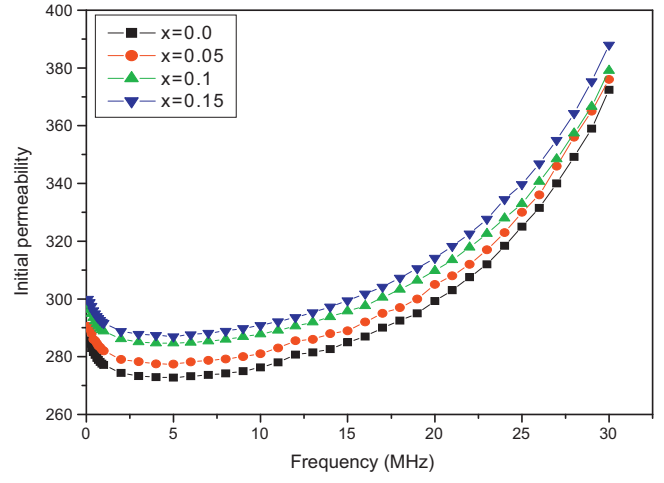

Fig. 6. Variation of initial permeability of $MgGd_xFe_{2-x}O_4$ (x = 0.0, 0.05, 0.1 and 0.15) ferrites with frequency measured at room temperature.

$$\mu_i = \frac{M_s^2 D_m}{K_1} \tag{10}$$

where D_m is the average grain diameter, K_1 is the magnetocrystalline anisotropy constant and M_s is the saturation magnetization. As μ_i is proportional to M_s^2, the variation of μ_i with x for Gd^{3+} should be affected in a manner similar to that of variation of M_s^2 with x. Hence the increase in initial permeability and saturation magnetization with Gd^{3+} ions concentration can be correlated well with each other. With an increase in Gd^{3+} ions concentration the resonance is observed at a lower frequency. This observation is in agreement with Snoek's law, according to which the resonance frequency (f_r) and the initial permeability (μ_i) are related as

$$\mu_i f_r = \text{constant}. \tag{11}$$

This shows that the higher the permeability values lower is the resonance frequency. The resonance of rotation magnetization caused by the action of the anisotropic field (H_a) can be calculated by using the following formula [20]

$$f_r = \frac{H_a \nu}{2\pi} \tag{12}$$

where ν is the gyromagnetic constant given by $\nu = 8.791 \times 10^6 g$ ($Oe^{-1}\,s^{-1}$), g is the gyromagnetic ratio. As the resonance occurs at higher frequencies for this ferrites, which leads to an extended zone of utility for these ferrites.

3.5. Relative loss factor

The variations of relative loss factor (RLF) of $MgGd_xFe_{2-x}O_4$ ferrites with frequency measured at room temperature are shown in Fig. 7. Relative loss factor (RLF) is expressed as the ratio of magnetic loss to the initial permeability, i.e.

$$\text{Relative loss factor} = \frac{\tan\ \delta}{\mu_i} \tag{13}$$

The loss is due to the lag of domain walls with respect to the applied alternating field and is attributed to imperfections in the lattice. The values of RLF are observed to decrease initially with frequency, reaching a minimum value, and then become almost constant up to 20 MHz. The decrease in relative loss factor with increasing frequency is due to the fact that beyond certain frequency of the electric field, the domain wall motion cannot follow the applied electric field. The increase in relative loss factor above 20 MHz may indicate the beginning of a possible presence of resonance with peaks occurring at higher frequencies. At resonance, maximum energy is transferred from the applied field to the lattice resulting in the rapid increase in relative loss factor. It is clear from Fig. 7 that the relative loss factor is decreasing with an increase in Gd^{3+} ions content. As the RLF is inversely proportional to initial permeability and from Fig. 6 the initial permeability is increasing with an increase in Gd^{3+} ions content, so the RLF is found to be decreasing with increasing Gd^{3+} ions concentration. In ferrites, two resonance peaks are observed, one due to the domain wall oscillations at lower frequencies and the other due to Larmor precession of

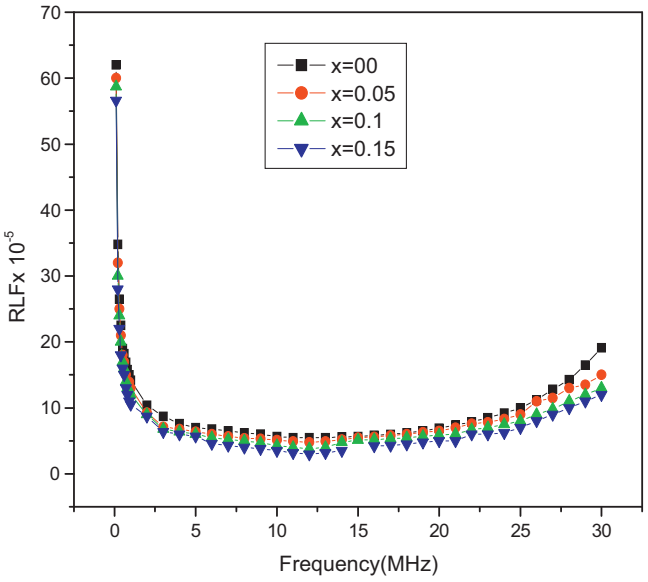

Fig. 7. Variation of relative loss factor of $MgGd_xFe_{2-x}O_4$ (x = 0.0, 0.05, 0.1 and 0.15) ferrites with frequency measured at room temperature.

electron-spins at higher frequencies. Low values of RLF are required for high frequency magnetic applications. The major contribution to the magnetic losses in ferrites is due to hysteresis losses, which in turn is based on damping phenomenon associated with irreversible wall displacement and spin rotations. However, the hysteresis loss becomes less important in the high-frequency range because the wall displacement is mainly damped and the hysteresis loss will be due to spin rotation. The values of relative loss factor are found to be small even at higher frequencies for these samples, which is one of the criteria for the materials to be used in microwave devices and for deflection yoke.

3.6. DC resistivity

Fig. 8 shows the variation of dc resistivity of $MgGd_xFe_{2-x}O_4$ ferrites with Gd^{3+} ions content (x) measured at room temperature. The value of dc resistivity increases with an increase in Gd^{3+} ions content (x). This is ascribed to two causes. One main cause is the increase in the porosity resulted from the doping of Gd^{3+} ions content in Mg ferrite. The other one is the addition of Gd^{3+} ions in place of Fe^{3+} ions limits the degree of conduction by blocking Verwey's hopping mechanism, resulting in an increase of resistivity. Fig. 9 shows the variation of dc resistivity of $MgGd_{0.15}Fe_{1.85}O_4$ ferrite with temperature. The dc resistivity of the sample decreases with increasing temperature according to Arrhenius equation [21]

$$\rho = \rho_o e^{E\rho/kT} \quad (14)$$

where E_ρ, k and T are the activation energy, Boltzmann's constant and the absolute temperature, respectively. The value of dc resistivity decreases with increase in temperature ensuring the semiconductor like behavior of the ferrites. With an increase in temperature of the ferrite will help the bound charges to be freed and participate in the conduction process, with the result of decreasing the resistivity.

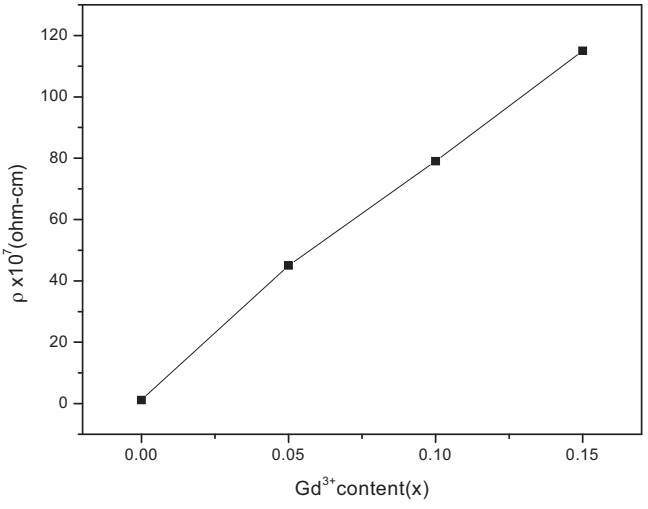

Fig. 8. Variation of dc resistivity of $MgGd_xFe_{2-x}O_4$ ferrites with Gd^{3+} ions content (x) measured at room temperature.

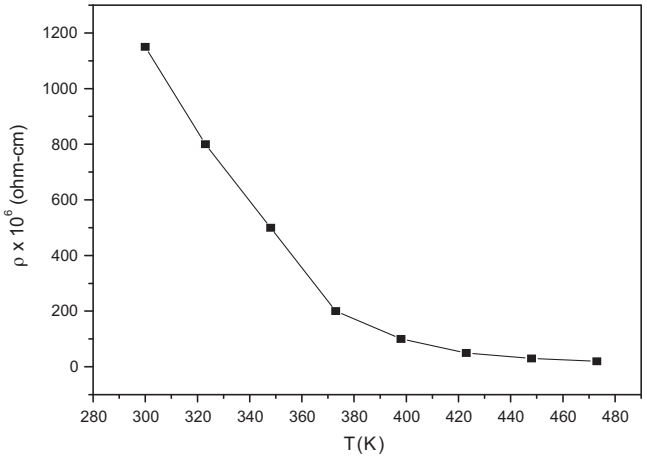

Fig. 9. Variation of dc resistivity of $MgGd_{0.15}Fe_{1.85}O_4$ ferrite with temperature.

3.7. Dielectric properties

Fig. 10 shows the variation of dielectric loss with frequency measured at room temperature. The dielectric loss factor decreases initially with an increase in frequency followed by the appearance of the resonance [22–24] with peaks occurring at higher frequencies. The decrease in dielectric loss with an increase in frequency can be explained on the basis of Koop's phenomenological model

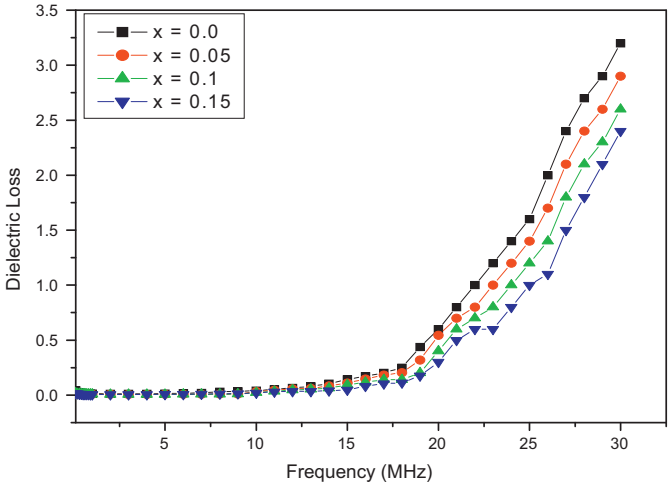

Fig. 10. Variation of dielectric loss of $MgGd_xFe_{2-x}O_4$ (x = 0.0, 0.05, 0.1 and 0.15) ferrites with frequency measured at room temperature.

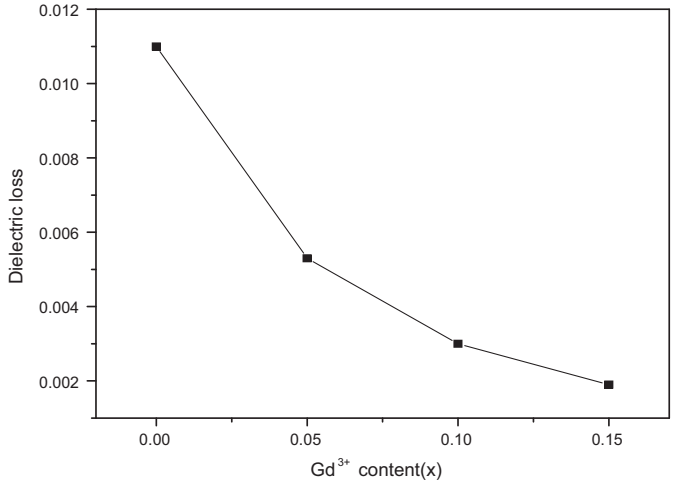

Fig. 11. Variation of dielectric loss of $MgGd_xFe_{2-x}O_4$ ferrites with Gd^{3+} ions content (x) measured at room temperature.

[25]. Resonance occurs when the frequency of the applied electric field is equal to hopping frequency.

Fig. 11 shows the variation of dielectric loss of $MgGd_xFe_{2-x}O_4$ ferrites with Gd^{3+} ions content (x) measured at room temperature. The dielectric loss factor decreases with an increase in Gd^{3+} ions content (x). The porosity is found to be increasing with an increase in Gd^{3+} ions content in $MgFe_2O_4$ ferrite. Higher porosity results in lower dielectric losses. Husdon [26] has shown that the dielectric losses in ferrites is reflected in the conductivity measurements where the materials of high conductivity exhibiting higher losses and vice versa.

Fig. 12 shows the variation of dielectric constant as a function of frequency measured at room temperature. The dielectric constant decreases initially with an increase in frequency followed by the appearance of the resonance with peaks occurring at higher frequencies. Dielectric constant is due to the polarization of the material. The decrease of polarization with increasing frequency is due to the fact that beyond certain frequency of the electric field, the electronic exchange between Fe^{2+} and Fe^{3+} ions cannot follow the electric field. These variations can be explained on the basis of space charge polarization model of Maxwell–Wagner [27,28]

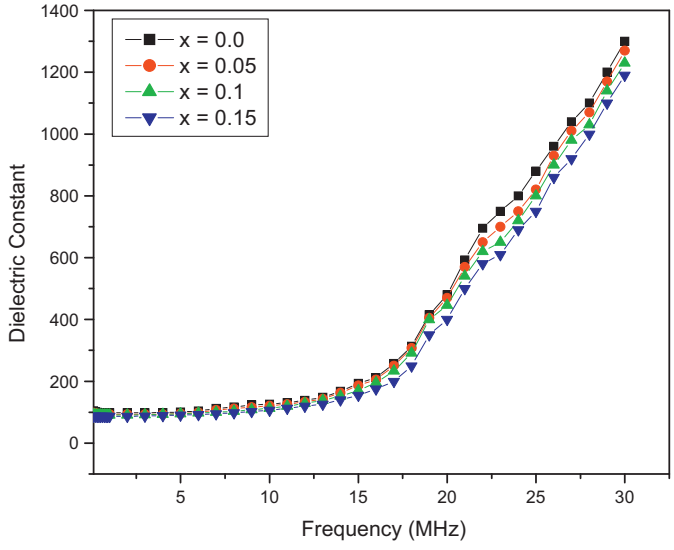

Fig. 12. Variation of dielectric constant of $MgGd_xFe_{2-x}O_4$ (x = 0.0, 0.05, 0.1 and 0.15) ferrites with frequency measured at room temperature.

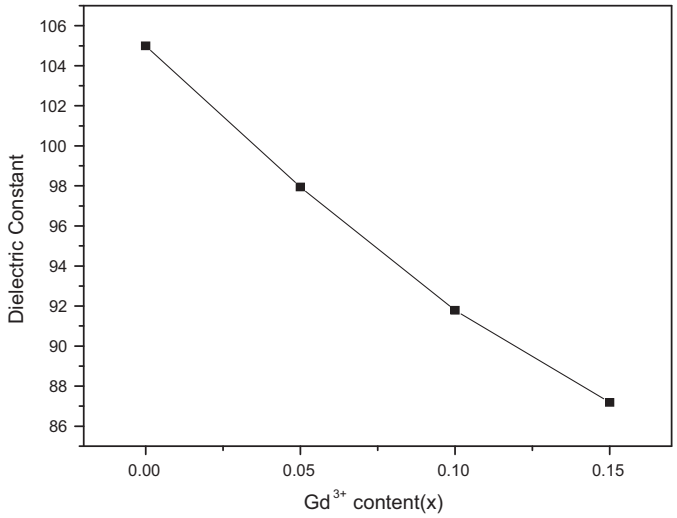

Fig. 13. Variation of dielectric constant of $MgGd_xFe_{2-x}O_4$ ferrites with Gd^{3+} ions content (x) measured at room temperature.

in agreement with the phenomenon of dipole relaxation [29,30]. The resonance may occur when the frequency of charge transfer between $Fe^{2+} \leftrightarrow Fe^{3+}$ ions is equal to that of the applied electric field.

Fig. 13 shows the variation of dielectric constant of $MgGd_xFe_{2-x}O_4$ ferrites with Gd^{3+} ions content (x) measured at room temperature. The dielectric constant decreases with an increase in Gd^{3+} ions content (x). This is ascribed to two causes. One main cause is the increase in the porosity resulted from the doping of Gd^{3+} ions content in Mg ferrite. Higher porosity results in lower dielectric constant. The other can be explained in view of the hopping conduction mechanism between $Fe^{2+} \leftrightarrow Fe^{3+} + e^{-1}$, the addition of Gd^{3+} ions in place of Fe^{3+} ions limits the degree of conduction and polarization by blocking Verwey's hopping mechanism, results in the decrease of conductivity and dielectric constant [31–34].

4. Conclusions

$MgGd_xFe_{2-x}O_4$ (x = 0.0, 0.05, 0.1 and 0.15) ferrites were successfully synthesized by solid state reaction technique. The values of dc resistivity have been increased from 1.12×10^7 (Ω cm) to 1.15×10^9 (Ω cm) due to the doping of Gd^{3+} ions in Mg ferrite. Incorporation of Gd^{3+} ions results in an increase in initial permeability, saturation magnetization and remnant magnetization. Saturation magnetization has been increased by two times and remnant magnetization has been increased by more than three times due to the doping of Gd^{3+} ions in Mg ferrite. The values of RLF in the presently studied ferrites at room temperature are of the order of 10^{-4}–10^{-5}. Low values of RLF exhibited by these ferrites suggest its utility in inductor and transformer applications.

Acknowledgements

S.K.S. and M.K. are thankful to FAPESP (Process No. 06/06792-2) and CNPq, Brazil for providing financial support.

References

[1] M.S. Khandekar, R.C. Kambale, J.Y. Patil, Y.D. Kolekar, S.S. Suryavanshi, J. Alloys Compd. 509 (2011) 1861–1865.
[2] A. Pradeep, P. Priyadharsini, G. Chandrasekaran, J. Alloys Compd. 509 (2011) 3917–3923.
[3] M. Atif, M. Nadeem, R. Grossinger, R. Sato Turtelli, J. Alloys Compd. 509 (2011) 5720–5724.

[4] C. Venkataraju, G. Sathishkumar, K. Sivakumar, J. Magn. Magn. Mater. 323 (2011) 1817–1822.
[5] M. Anis-ur-Rehman, M.A. Malik, M. Akram, K. Khan, A. Maqsood, Phys. Scr. 83 (2011) 015602.
[6] J. Chand, M. Singh, J. Alloys Compd. 486 (2009) 376–379.
[7] Amarendra K. Singh, A.K. Singh, T.C. Goel, R.G. Mendiratta, J. Magn. Mater. 281 (2004) 276.
[8] R.K. Sharma, O. Suwalka, N. Lakshmia, K. Venugopalana, A. Banerjeeb, P.A. Joyc, Mater. Lett. 59 (2005) 3402–3405.
[9] A. Lakshman, K.H. Rao, R.G. Mendiratta, J. Magn. Magn. Mater. 250 (2002) 92.
[10] S.H. Keluskar, R.B. Tangsali, G.K. Naik, J.S. Budkuley, J. Magn. Magn. Mater. 305 (2006) 296.
[11] A. Verma, T.C. Goel, R.G. Mendiratta, M.I. Alam, Mater. Sci. Eng. B 60 (1999) 156–162.
[12] S. Thakur, S.C. Katyal, A. Gupta, V.R. Reddy, M. Singh, J. Appl. Phys. 105 (2009), 07A521-3.
[13] C.-s. Wang, X.-f. Gu, Y.-g. Sun, E.-j. Gao, W.-z. Zhang, Chem. Res. Chin. Univ. 25 (5) (2009) 614–619.
[14] R.N. Bhowmik, R. Ranganathan, J. Magn. Magn. 248 (2002) 101.
[15] F. Gozuak, Y. Koseoglu, A. Baykal, H. Kavas, J. Magn. Magn. 321 (2009) 2170–2177.
[16] L. Neel, Ann. Phys. Paris 3 (1948) 137–198.
[17] J. Gieraltowski, A. Globus, IEEE Trans. Magn. 13 (1977) 1359.
[18] A. Globus, J. Phys. (Paris) Colloq. 38 (1977) 1.
[19] A. Globus, P. Duplex, M. Guyot, IEEE Trans. Magn. Magn. 7 (1991) 617.
[20] S.-H. Kang, H.-I. Yoo, J. Appl. Phys. 88 (2000) 4754.
[21] J. Smit, H.P.J. Wijn, Ferrites, Philips Technical Library, Eindhoven, The Netherlands, 1959.
[22] S. Thakur, S.C. Katyal, M. Singh, Appl. Phys. Lett. 91 (2007) 262501.
[23] K. Singh, N.S. Negi, R.K. Kotnala, M. Singh, Solid State Commun. 148 (2008) 18–21.
[24] P. Kumar, S.K. Sharma, M. Knobel, M. Singh, J. Alloys Compd. 508 (2010) 115–118.
[25] C.G. Koops, Phys. Rev. 83 (1951) 121.
[26] A.S. Husdon, Marconi Rev. 37 (1968) 43.
[27] J.C. Maxwell, Electricity & Magnetism, vol. 1, Oxford University Press, Oxford, 1929, Section 328.
[28] K.W. Wagner, Ann. Phys. (Leipzig) 40 (1913) 817.
[29] D.H. Wang, W.C. Goh, M. Ning, C.K. Ong, Appl. Phys. Lett. 88 (2006) 212907.
[30] M. Kumar, K.L. Yadav, J. Appl. Phys. 100 (2006) 74111.
[31] M.A. Ahmed, E. Ateia, F.M. Salem, J. Mater. Sci. 42 (2007) 3651–3660.
[32] S. Kumar, Alimuddin, R. Kumar, P. Thakur, K.H. Chae, B. Angadi, W.K. Choi, J. Phys. Condens. Matter. 19 (2007) 476210.
[33] A.V. Ramana Reddy, G. Ranga Mohan, D. Ravinder, J. Matter. Sci. 34 (1999) 3169.
[34] M.A. Ahmed, E. Ateia I, EL-DEKS Vib. Spectrosc. 30 (2002) 69–75.